Numerical Modeling of Field Tests in Unsaturated Fractured Basalt at the Box Canyon Site

Christine Doughty
Earth Sciences Division
E.O. Lawrence Berkeley National Laboratory

Abstract

A TOUGH2 model of a ponded infiltration test has been developed and used to predict the results of a field experiment conducted in the vadose zone of the fractured Snake River Plain basalts, at the Box Canyon site in southeastern Idaho. The key question addressed is how fracture-pattern characteristics and connectivity affect the pattern of liquid infiltration. The numerical model, a two-dimensional vertical cross-section, uses half-meter discretization for the shallow field site, which extends about 20 m from the ground surface to an underlying perched water body. The model includes explicit but highly simplified representations of major fractures and other important hydrological features. It adequately reproduces the majority of the field observations, confirming the notion that infiltration is largely fracture-controlled.

1. Introduction

E.O. Lawrence Berkeley National Laboratory (Berkeley Lab), in collaboration with Idaho National Engineering and Environmental Laboratory (INEEL) and Stanford University, is involved in an ongoing project to study flow and transport in fractured basalt vadose zones, for the purpose of improving performance of environmental remediation activities in such environments, and to develop improved monitoring techniques for both fundamental studies and remediation actions. Field work is conducted at Box Canyon, located near INEEL in the Eastern Snake River Plain, Idaho. At the Box Canyon site, a clean site designed to serve as an analog for contaminated sites located within INEEL, a 20 by 20 m well field consisting of 35 vertical and slanted boreholes has been developed, and a 7 by 8 m infiltration pond has been constructed. A nearby cliff-face exposure of the fractured basalts and minimal soil cover provide excellent views of the basalt flow structure, enabling extensive geologic mapping.

Field tests conducted at the Box Canyon site include hot air injection tests (Long et al., 1995), cross-hole air interference tests, and ponded infiltration tests (Faybishenko et al., 1998). The present paper describes mathematical modeling conducted prior to the first ponded infiltration test using TOUGH2 (Pruess, 1987, 1991). Simulations were conducted prior to the field test to aid in experimental design, to study the importance of different factors affecting the test, and to predict the results of the test in order to assess our understanding of the salient features of flow and transport in a fractured vadose zone. Simulations were also conducted after the field test to help explain the observed results, to assess the adequacy of the conceptual and numerical models, to infer the importance of various physical processes and the values of material properties, and to help design future tests.

One of the key questions to be addressed by modeling studies is how fracture-pattern characteristics and connectivity affect the pattern of water infiltration. For example, will flow occur predominantly through fractures or will matrix flow be significant? Is vertical connectivity great enough to allow purely vertical infiltration with little lateral spreading, or will extensive spreading occur? The deterministic modeling approach was chosen over the more traditional stochastic approach to represent heterogeneity because there is a great deal known about the formation process and resulting geometric structure of the fracture patterns for the Snake River Plain basalts (e.g., Aydin and Lore, 1997; Grossenbacher and Faybishenko, 1998). Available random field generators, even those which allow multiple anisotropic correlation scales, are not likely to capture the features of fracture connectivity that we believe are essential for modeling liquid infiltration and transport realistically. Flow and transport through heterogeneous media may be studied at a variety of scales, ranging from laboratory to regional, and the choice of modeling approach will certainly depend on the scale of interest. At the intermediate field scale of the Box Canyon site (tens of meters), we feel that we know enough about the hydrogeologic setting to be comfortable treating it deterministically.

2. Model Development

Figure 1 shows a schematic geologic cross-section through the Box Canyon site, which identifies the principal hydrogeologic components. The model for the ponded infiltration test is a two-dimensional vertical cross-section that extends from the ground surface to a depth of 20 m, the approximate depth of a local perched water body. It is comprised of an upper basalt flow, shown in Figure 1, an underlying rubble zone, and the upper portion of a lower basalt flow. The model underlies the NE-SW diagonal (10 m

length) of the infiltration pond, and extends beyond the pond 5 m on both sides. The model includes explicit representations of features observed in boreholes such as soil infilling in shallow fractures, lens-shaped vesicular zones between depths of 0 and 6 m, a central horizontal fracture zone at a depth of about 7 m, a sparsely-fractured massive basalt between depths of 7 and 10 m, and a vesicular zone overlying a rubble zone at a depth of about 10 m. Some of these features are shown in Figure 1. Low- and high-permeability layers inferred from the results of the hot air injection test are also included in the model. Additionally, the model incorporates the general pattern of column-bounding and column-normal fractures whose spacing increases with distance from the top and bottom edges of the basalt flow, by copying the pattern mapped at the cliff-face exposure of the upper basalt flow in Box Canyon (Figure 2). A hierarchical structure has been developed to categorize the fractures (B. Faybishenko, personal communication), and fracture permeability values are assigned based on this structure, as given in Table 1. The material property distribution of the model is shown in Figure 3. The grid spacing is 0.5 by 0.5 m.

There are three significant limitations of the present representation of fractures within the vertical cross-section model. Firstly, although we believe that the general structure of the fracture pattern mapped at the Box Canyon cliff face represents the fracture pattern underlying the infiltration pond correctly, specific locations for individual fractures are very likely to be wrong. This is because the distance from the cliff face to the infiltration pond is about 25 m, whereas the maximum extent of fractures perpendicular to the cliff face is probably less than 5 m (the maximum observed fracture spacing along the cliff face is about 5 m and the fracture pattern is expected to be isotropic in plan view). Therefore, the model cannot make detailed predictions for individual point observations. It can, however, be used to predict behavior at 'generic' locations, for example the time-dependence of wetting for a location adjacent to a primary vertical fracture. The model can also be used to study the effect of different parameters and processes on the spatial variability of the infiltration process.

Secondly, although the model is finely enough discretized to label individual grid blocks as either representing a fracture or matrix (grid block dimension 0.5 m, with fracture spacing ranging from 0.5 to 5 m), it cannot locate fractures more precisely than within the 0.5 m grid block width. The model does not allow a rigorous treatment of flow within a fracture, in which apertures probably range from microns to millimeters, or fracture/matrix interactions, which require fine discretization of the matrix adjacent to the fractures. Instead, an effective continuum approach is used, in which grid blocks that represent fractures actually encompass the 0.5 m wide zone of basalt in which the fracture lies. The grid block is assigned a large permeability to account for flow through the fracture and a small porosity to account for the small aperture of the fracture.

Thirdly, there are problems associated with representing a three-dimensional fracture network with a two-dimensional model. In general, water becomes trapped more easily in a two-dimensional model because the connectivity of the model is too low.

3. Model Application

Processes Modeled

Two alternative approaches were taken to model the ponded infiltration test. The first uses the traditional soil physics approach, in which air is a passive spectator, and liquid saturation is the only variable to be calculated. The EOS9 module of TOUGH2 implements this approach (Wu et al., 1996). The second, more rigorous, approach is to consider the fully coupled two-phase flow of water and air, which can be done using the EOS3 module of TOUGH2, and requires calculating both gas pressure and liquid saturation. The primary motivation for using EOS9 is numerical efficiency. The addition of air to infiltration problems can cause severe numerical difficulties, especially for highly heterogeneous media, because the physical processes occur on very different time scales. The primary motivation for using EOS3 is that it allows the development of entrapped air, which is believed to be an important effect for infiltration into heterogeneous media (Faybishenko, 1993, 1995).

Corey (1954) curves are used to describe relative permeability as a function of liquid saturation. Capillary pressure is set to zero in most of the pre-test calculations. This is done because there is no real data to specify what kind of capillary pressure-liquid saturation relations are appropriate for the fractured basalts at Box Canyon, although fracture capillary pressure strength is commonly assumed to be small. Generally, flow paths and moisture distributions develop in response to a combination of capillary and gravity forces, with gravity acting to localize flow to high-permeability pathways and capillary forces

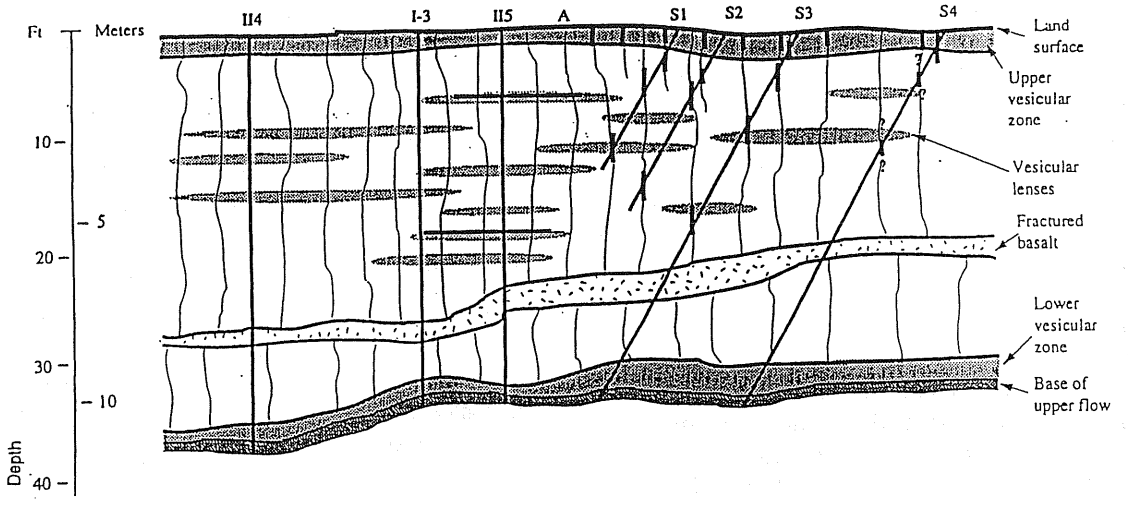

Figure 1. A schematic geologic cross-section through the Box Canyon field site, showing the upper of the two basalt flows modeled. The base of the flow is the upper boundary of the rubble zone (after Long et al., 1995).

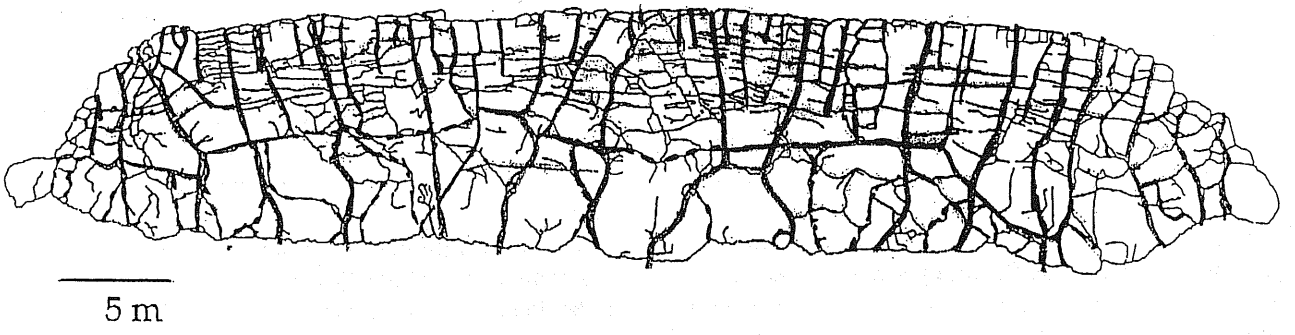

Figure 2. Fracture pattern in the upper basalt flow mapped at the Box Canyon cliff face exposure near the ponded infiltration test site (after Aydin and Lore, 1997). Primary (through-going) vertical fractures are shown bold.

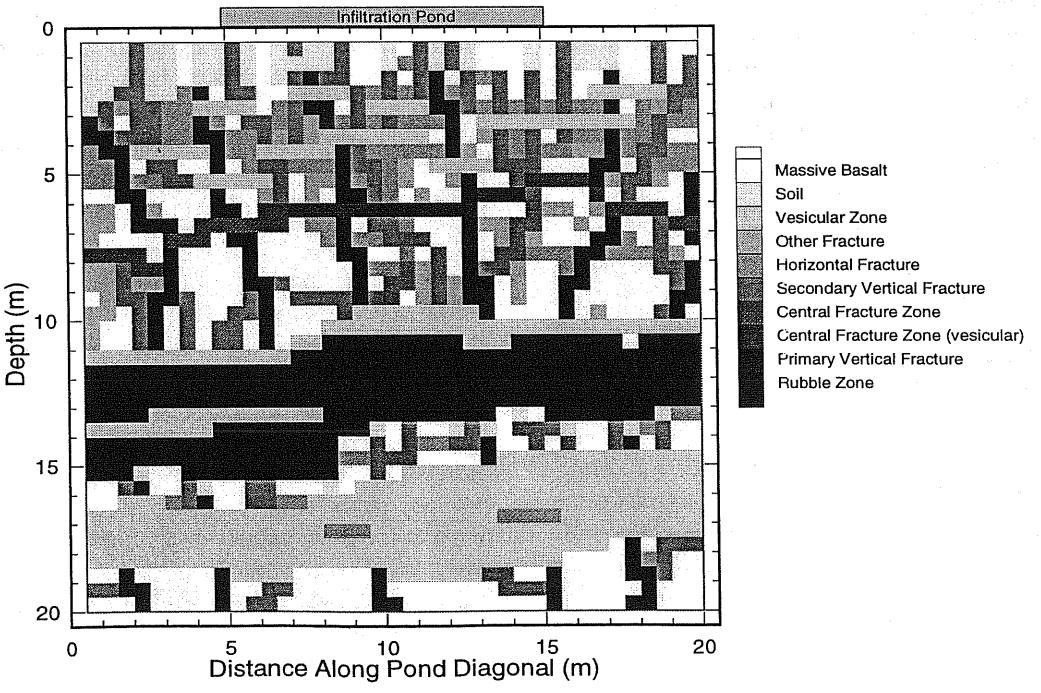

Figure 3. Two-dimensional vertical cross-section model used for the ponded infiltration test.

spreading moisture to low-permeability regions diffusively. By ignoring capillary forces, we produce a sharper picture of preferential flow paths than is likely to exist in the field. Ultimately, we hope to use the results of laboratory and field infiltration tests, in conjunction with inverse modeling, to infer appropriate characteristic curves for the Box Canyon site.

Initial and Boundary Conditions

For the EOS9 calculations, the initial condition is a uniformly partially-saturated medium with $S_l = 0.1$, in which water is immobile ($S_{lr} = 0.12$). For the EOS3 calculations, a gas-static pressure profile is also specified.

The pond boundary is represented by a liquid-saturated, constant-pressure boundary at 0.3 m of head. For the EOS3 calculations, a constant-pressure boundary representing the atmosphere overlies the non-pond portion of the model upper boundary, whereas for the EOS9 calculations this is a closed boundary. Lateral and lower boundary conditions are constant saturation (and constant pressure for EOS3). Lateral boundaries are open to liquid flow (and gas flow for EOS3) and the lower boundary, which represents a local perched water body, is open to liquid flow. Ponding lasts for four weeks.

Simulation Results

Two simulations were done, one with EOS9 and one with EOS3. The predicted saturation distributions and liquid flow fields at a series of times are shown in Figures 4 and 5 for the EOS9 and EOS3 cases, respectively. In both cases, the infiltration does not proceed uniformly, but follows highly irregular paths, bypassing the massive basalt sections, and focusing in the high-permeability fractures. A moderate amount of lateral spreading occurs, with the plume width increasing from the pond width of 10 m to about 15-18 m near the bottom of the model. The primary avenues for lateral flow are vesicular lenses and the central fracture zone. Flow through most of the rubble zone (11-14 m depths) is purely vertical, with lateral spreading occurring only in limited zones along the bottom margin.

Figure 6 compares the observed pond outflow rate with the simulated values for the two cases. For the model, pond outflow is entirely due to infiltration, whereas for the observed data it includes both infiltration and evaporation, which is estimated to be about 1-2 cm/day). The general time variation of pond outflow rate is reproduced in both cases, but the simulations show a smaller overall decrease in outflow rate. The early-time under-prediction of outflow rate may arise because of leaks that existed in the pond during the first few days of the test, resulting in a larger area available for infiltration than in the models. The late-time over-prediction of outflow rate may be the result of decreases in permeability caused by clogging of flow paths by fine materials, which is not included in the model.

The EOS3 simulation yields significantly different results than does the EOS9 simulation, suggesting that entrapped air plays an important role, and needs to be included in the model. Although the infiltrating water generally finds the same preferential pathways for the EOS9 and EOS3 simulations (compare Figures 4 and 5), more regions are bypassed and the saturation distribution is much less uniform when entrapped air develops. Subsurface flow rates are also smaller, due to the countering of gravity forces by pressure gradients caused by the development of entrapped air. The pond outflow rate is consequently smaller as well.

4. Conclusions

The modeling studies suggest that infiltration will not occur uniformly, but will follow irregular flow paths through the highest-permeability features. Some lateral spreading is expected through vesicular zones and the central fracture zone, but flow through the rubble zone is expected to be nearly vertical. Entrapped air is expected to have an important effect. Although the present model does not include capillary forces, a sensitivity study suggests that while capillary forces tend to smooth the distribution of water in the subsurface, they are not the primary factor controlling pathways through the subsurface or outflow rate from the pond. Overall, the model results have been consistent with field observations, and modeling has been an effective tool to assess and improve our understanding and aid in experimental design.

Acknowledgements

The careful review of this work by S. Finsterle and B. Faybishenko is greatly appreciated. This work was supported by the Assistant Secretary for Environmental Restoration and Waste Management, EM-50, Office of Technology Development, Characterization, Monitoring and Sensor Technology Program, of the U.S. Department of Energy under Contract No. DE-AC03-76SF00098.

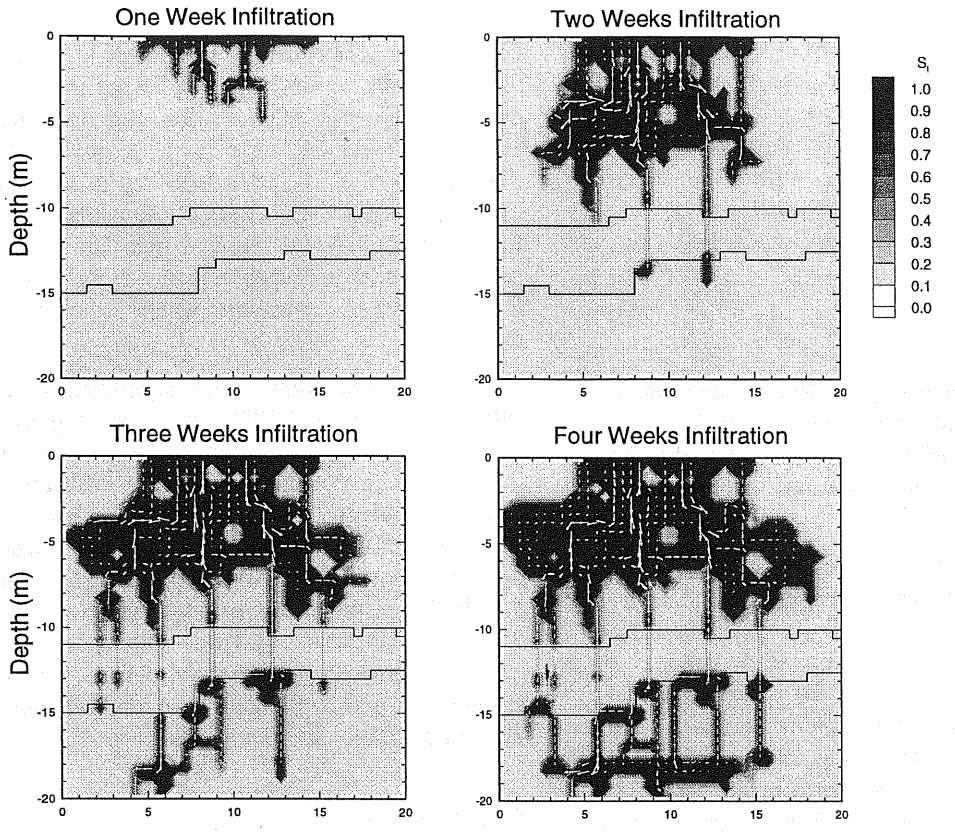

Figure 4. Simulated liquid saturation distribution and liquid flow field during the infiltration test, for the EOS9 case. The injection pond and rubble zone boundaries are also shown.

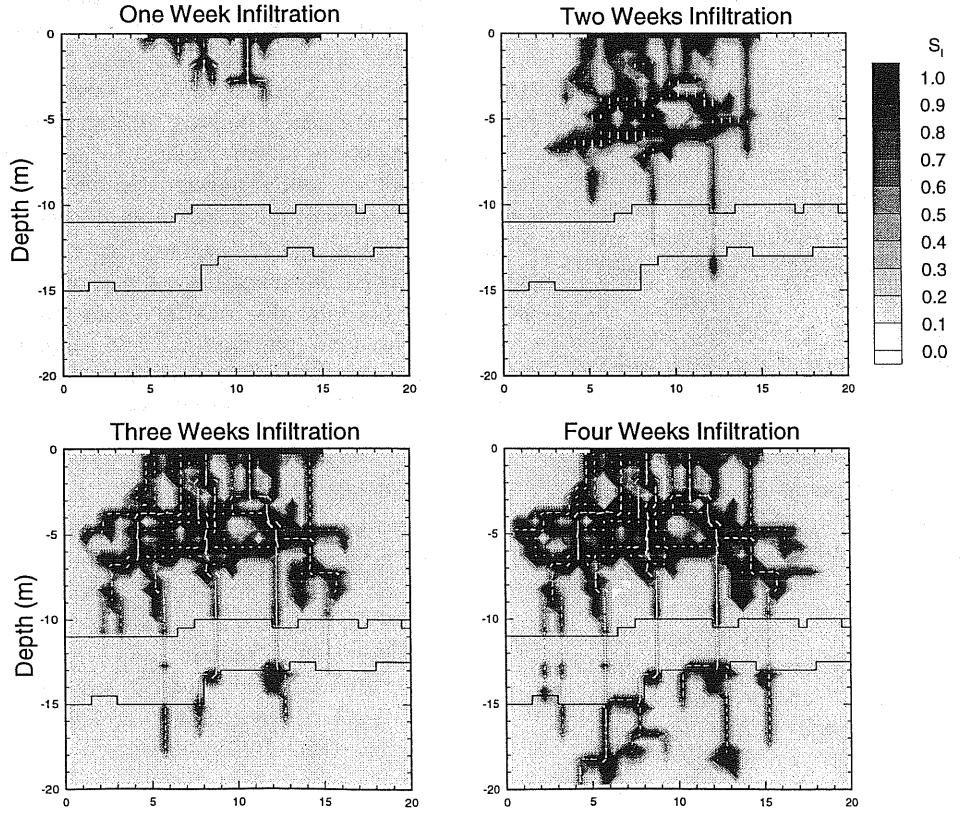

Figure 5. Simulated liquid saturation distribution and liquid flow field during the infiltration test, for the EOS3 case.

References

Aydin, A. and J. Lore, Characterization of the fracture patterns in basalt flows at Box Canyon, Idaho, internal report, Lawrence Berkeley National Laboratory, Berkeley, CA, 1997.

Baca, R.G., S.O. Magnuson, H.D. Nguyen, and P. Martian, A modeling study of water flow in the vadose zone beneath the Radioactive Waste Management Complex, Rep. EGG-GEO-10068, Idaho National Engineering Laboratory, Idaho Falls, Idaho, 1992

Bishop, C.W., Hydraulic properties of vesicular basalt, M.Sc. Thesis, Dept. of Hydrology and Water Resources, University of Arizona, Tucson, AZ, 117 pp., 1991.

Corey, A.T., The interrelation between gas and oil relative permeabilities, Producers Monthly, 19, 38-41, 1954.

Faybishenko, B., Two field experiments for ponded infiltration in foundation pits, presented at AGU 13th Annual Hydrology Days, Colorado State University, Fort Collins, Colorado, March 30-April 2, 1993.

Faybishenko, B.A., Hydraulic behavior of quasi-saturated soils in the presence of entrapped air: laboratory experiments, Water Resources Res., 31(10), 2421-2435, 1995.

Faybishenko, B. et al., Ponded infiltration test at the Box Canyon site: data report and preliminary analysis, Rep. LBNL-40183, Lawrence Berkeley National Laboratory, Berkeley, CA, 1998.

Grossenbacher, K.A. and B. Faybishenko, Spacing of thermally induced columnar joints in basalt: variation with depth, Lawrence Berkeley Laboratory Report, 1998.

Knutson, C.F., K.A. McCormick, J.C. Crocker, M.A. Glenn, and M.L. Fishel, 3D RWMC vadose zone modeling, Rep. EGG-RD-10246, Idaho National Engineering Laboratory, Idaho Falls, Idaho, 1992.

Long, J.C.S., C. Doughty, B. Faybishenko, et al., Analog site for fractured rock characterization, Annual Report FY 1995, Lawrence Berkeley National Laboratory Report LBL-38095, October, 1995.

Pruess, K., TOUGH user's guide, Rep. LBL-20700, Lawrence Berkeley Laboratory, Berkeley, CA, 1987.

Pruess, K., TOUGH2 - A general-purpose numerical simulator for multiphase fluid and heat flow, Rep. LBL-29400, Lawrence Berkeley Laboratory, Berkeley, CA, 1991.

Wu, Y.S., C.F. Ahlers, P. Fraser, A. Simmons and K. Pruess, Software qualification of selected TOUGH2 modules, Rep. LBNL-39490, Lawrence Berkeley National Laboratory, Berkeley, CA, 1996.

Table 1. Material properties used for the TOUGH2 simulations of the ponded infiltration test.

Material	Porosity	Horizontal Permeability (10^{-15} m^2)	Vertical permeability (10^{-15} m^2)
Rubble zone	0.50	10^6	10^6
Primary vertical fractures	0.08	50	5000
Central fracture zone (vesicular)	0.15	5000	50
Central fracture zone (non-vesicular)	0.10	5000	50
Secondary vertical fracture (Knutson et al., 1992)	0.07	0.05	500
Horizontal fracture	0.05	5000	0.05
Other fracture	0.05	50	50
Vesicular basalt (Bishop, 1991)	0.20	1000	1000
Soil (Baca et al., 1992)	0.50	78	78
Massive basalt	0.05	0.05	0.05

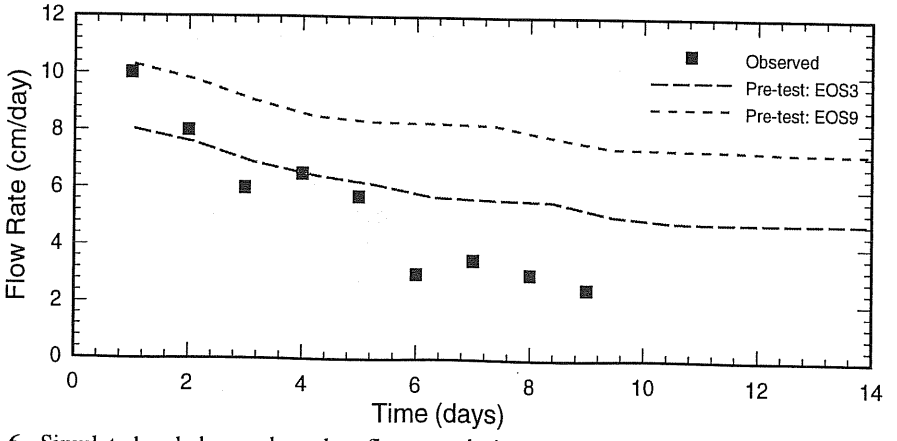

Figure 6. Simulated and observed pond outflow rate during the ponded infiltration test.